EPJ manuscript No.
(will be inserted by the editor)

Random Delayed-Choice Quantum Eraser via Two-Photon Imaging

Giuliano Scarcelli[1,2a], Yu Zhou[1], and Yanhua Shih[1]

[1] Department of Physics, University of Maryland, Baltimore County, Baltimore, Maryland 21250
[2] Dipartimento Interateneo di Fisica, Universita' di Bari, 70126, Bari, Italy

Received: date / Revised version: date

Abstract. We report on a delayed-choice quantum eraser experiment based on a two-photon imaging scheme using entangled photon pairs. After the detection of a photon which passed through a double-slit, a random delayed choice is made to erase or not erase the which-path information by the measurement of its distant entangled twin; the particle-like and wave-like behavior of the photon are then recorded simultaneously and respectively by only one set of joint detection devices. The present eraser takes advantage of two-photon imaging. The complete which-path information of a photon is transferred to its distant entangled twin through a "ghost" image. The choice is made on the Fourier transform plane of the ghost image between reading "complete information" or "partial information" of the double-path.

PACS. PACS-key discribing text of that key – PACS-key discribing text of that key

1 Introduction

Quantum erasure was proposed in 1982 by Scully and Druhl [1]. After two decades the subject has become one of the most intriguing topics in probing the foundations of quantum mechanics [2,3]. The idea of quantum erasure lies in its connection to Bohr's principle of complementarity [4]: although a quantum mechanical object is dually particle and wave; its particle-like and wave-like behaviors cannot be observed simultaneously. For example, if one observes an interference pattern from a standard Young's double-slit interferometer by means of single-photon counting measurement, a photon must have been passing both slits like a wave and consequently the which-slit information can never be learned. On the other hand, any information about through which slit the photon has passed destroys the interference. In this context Scully and Druhl showed that if the which-slit (which-path) information is erased, the interference pattern can be recovered; the situation becomes extremely fascinating when the erasing idea is combined with the delayed choice proposal by Wheeler and Alley [5,6]: i.e. even after the detection of the quantum itself, it is still possible to decide whether to erase or not to erase the which-path information, hence to observe the wave behavior or the particle behavior of the quantum mechanical object.

In the past two decades, a number of experiments demonstrated the quantum eraser idea by means of different experimental approaches and/or different point of theoretical concerns [7,8,9,10,11,12,13,14,15,16,17]; in particular Kim et al. [12] have realized an experiment very close to the original proposal by using entangled photon pair of spontaneous parametric down-conversion (SPDC). The experiment demonstrated that the which-path information of a photon passing through a double-slit can be erased at-a-distance by its entangled twin even after the annihilation of the photon itself. The choice was made between the joint detection of a single two-photon amplitude that involved either the upper slit or the lower slit (read which-path information) or the joint detection of a pair of indistinguishable two-photon amplitudes involving both slits (erase which-path information).

Unlike all previous experiments the present work takes advantage of two-photon imaging. A photon passes through a standard Young's double-slit for its complementarity examination. The quantum correlation between this photon and its entangled twin allows the formation of a "ghost" image of the double-slit on the side of the entangled twin. Thus, the which path information is completely passed to the entangled twin photon and can be erased by the detection of the twin. After the detection of the photon which passed through the double-slit, a random choice is made on the Fourier transform plane of the "ghost" image between "reading complete information" or "reading partial information" of the double path. Inherently, this new approach can be easily extended to multiple paths or arbitrary continuous spatial modulations.

Any attempt to interpret the physics of the quantum eraser in terms of complementarity examination on a sin-

[a] *Present address:* Harvard Medical School and Wellman Center for Photomedicine, Massachusetts General Hospital, Boston Ma 02114, gscarcelli@partners.org

gle photon leads to counterintuitive results and paradoxical conclusions; on the other hand, if the two-photon nature of the phenomenon is accepted, a straightforward explanation of the observed effect can be given through Klyshko's interpretation of two-photon geometric optics. From a new angle it is emphasized that the physics behind two-photon phenomena is significantly different from that of two independent photons[18].

In this context another novelty of our experiment is particularly important: a new type of detection scheme. In all previous quantum erasers, the observation or not observation of the interference pattern were associated to different experiments, or at least to different photoelectric detectors. Therefore even though the physics behind the erasure has been exploited, the implementation of the random delayed choice can still be improved. In our realization both the erasing choice and the reading choice are analyzed by a single detector. This characteristic stresses the interpretative difficulties of the quantum eraser. In fact in our experiment the particle-like and wave-like behavior of the photon are recorded randomly and simultaneously by the same pair of joint measurement devices in only one measurement process.

The nearly equivalent experimental conditions in which the realization of the different choices occurs fully implement Wheeler and Alley delayed-choice proposal and therefore raise troubling questions on where the measurement, hence the collapse of the wave function, occurs. The validity of Bohr's principle of complementarity is probed in a deeper way than in previous experiments.

The paper is organized as follows: in section II, the principle behind our quantum eraser is explained and its connection to the intriguing physics of quantum imaging; in section III, a mathematical derivation resulting in the experimental observation is provided with a brief discussion of attempted interpretations with their difficulties; in section IV, the experimental setup and results are described in detail; and finally in section V, some conclusive remarks are presented.

2 Quantum imaging

The quantum eraser here reported uses the fascinating physics of quantum imaging. The study of quantum imaging started ten years ago after the first demonstration of an imaging experiment that used entangled two-photon state of spontaneous parametric down-conversion [19,20]. In that experiment, the signal photon of SPDC passed through an imaging lens and a complicated aperture, while the idler photon propagated freely; nevertheless the complete spatial distribution information was present in the idler photon side of the setup and an image (named "ghost" because even though it was formed by the idler radiation, it reconstructed the spatial modulation experienced only by the signal radiation) was formed in a plane satisfying a Gaussian thin lens equation involving both arms of the setup. Over the past ten years, quantum imaging has attracted a great deal of attention. The equivalence between two-photon Fourier optics and classical Fourier optics, (with the replacement of the two-photon amplitudes leading to a joint detection by the spatial modes of the classical electric field) has been shown [21]. The two-photon amplitudes and their coherent superposition are troubling concepts in a classical sense because they imply a non-local behavior of the radiation; however, they explain in an elegant, consistent and intuitive way all the features of entangled two-photon optics.

The principle behind our realization of quantum erasure is illustrated in Fig. 1. The entangled signal and idler photons generated from SPDC are separated and directed to two photon counting detectors through two individual arms of an optical setup. In one arm the signal photon passes through a standard Young's double-slit interferometer; in the other arm, an imaging lens is used for the production of the equal size two-photon "ghost" image of the double-slit. There is an exact point-to-point correspondence between the plane of the slits x_o and the image plane x_I hence the information about the path of the signal photon in the double-slit plane is mapped onto the idler beam in the two-photon imaging plane. At this point we can choose to *erase* or to *read* such information to decide if the wave-like behavior, i.e., the interference pattern, of the photon is observable. To achieve this, a Fourier transform approach is employed as shown in Fig. 2. The two-photon image function $f(x_I)$, that contains the which-path information, is Fourier transformed by the lens L' onto its Fourier transform plane. On the Fourier transform plane, the photon counting detector D_2 either *reads* the full transformed function or *erases* most of it. Knowledge of all the coefficients of the Fourier expansion is sufficient to reconstruct the two-photon image function of the double-slit that means knowing the which-path information. On the other hand, if only the DC term of the Fourier expansion is read, it will never be possible to reconstruct the structure of the image function $f(x_I)$. Consequently, the which-path information of the signal photon is *erased*. Thus, the wave behavior will be learned by the observation of the interference.

The Fourier Transform approach to the quantum eraser is very interesting, it provides more flexibility in the scheme. Since we are transferring the which-path information through an image, one could avoid using a double-slit that only provides two possible paths. In principle an infinite number of paths or any spatial information can be transferred and subsequently read or erased.

3 Theory

In this section we will first show that the which-path information is indeed present in the two-photon imaging plane following the exemplar setup in Fig. 1 and then we will explain in detail the two ways of collecting the idler photons that, for the sake of clarity, we named *erasing* and *reading* conditions (see Fig. 2).

3.1 Mapping the which-path information in the "ghost" imaging plane

In quantum theory of photodetection, the probability of having a joint photodetection at two space-time points, $(\boldsymbol{r}_1, t_1)$ and $(\boldsymbol{r}_2, t_2)$, is governed by the second order Glauber correlation function [22]:

$$G^{(2)}(t_1, \boldsymbol{r}_1; t_2, \boldsymbol{r}_2) \equiv \langle E_1^{(-)}(t_1, \boldsymbol{r}_1) E_2^{(-)}(t_2, \boldsymbol{r}_2) E_2^{(+)}(t_2, \boldsymbol{r}_2) E_1^{(+)}(t_1, \boldsymbol{r}_1) \rangle. \tag{1}$$

where $E^{(-)}$ and $E^{(+)}$ are the negative-frequency and the positive-frequency field operators at space-time points $(\boldsymbol{r}_1, t_1)$ and $(\boldsymbol{r}_2, t_2)$ and the average is done over the state of the radiation. Ignoring the temporal part, the transverse electric field can be written as:

$$\boldsymbol{E}_1^{(+)}(\boldsymbol{x}_1) \propto \sum_{\boldsymbol{q}} g_1(\boldsymbol{x}_1; \boldsymbol{q}) \hat{a}(\boldsymbol{q}) \tag{2}$$
$$\boldsymbol{E}_2^{(+)}(\boldsymbol{x}_2) \propto \sum_{\boldsymbol{q}} g_2(\boldsymbol{x}_2; \boldsymbol{q}) \hat{a}(\boldsymbol{q})$$

where $\boldsymbol{x}_i$ is the transverse position of the i^{th} detector, $\boldsymbol{q}$ is the transverse component of the momentum, $\hat{a}(\boldsymbol{q})$ is the annihilation operator for the mode corresponding to $\boldsymbol{q}$ and $g_i(\boldsymbol{x}_i; \boldsymbol{q})$ is the Green's function associated to the propagation of the field from the source to the i^{th} detector.

As far as the radiation is concerned, the process of SPDC involves sending a pump laser beam into a nonlinear material. Occasionally, the nonlinear interaction leads to the annihilation of a high frequency pump photon and the creation of two lower frequency photons known as signal and idler that satisfy the phase-matching conditions [23,24]. The transverse part of the state of the signal-idler radiation produced by a CW laser can be simplified as follows:

$$|\psi\rangle \propto \sum_{\boldsymbol{q}, \boldsymbol{q}'} \delta(\boldsymbol{q} + \boldsymbol{q}') \hat{a}^\dagger(\boldsymbol{q}) \hat{a}^\dagger(\boldsymbol{q}') |0\rangle. \tag{3}$$

In this case the second order correlation function can be written as

$$G^{(2)}(\boldsymbol{r}_1, t_1; \boldsymbol{r}_2, t_2) = |\langle 0| E^{(+)}(\boldsymbol{r}_2, t_2) E^{(+)}(\boldsymbol{r}_1, t_1) |\psi\rangle|^2 \tag{4}$$

where $\langle 0|$ denotes the vacuum state and $|\psi\rangle$ the two photon state of SPDC. $\langle 0| E^{(+)}(\boldsymbol{r}_2, t_2) E^{(+)}(\boldsymbol{r}_1, t_1) |\psi\rangle$ is an effective two-photon wavefunction, often referred to as *biphoton.*

While in classical optics intensities are measured, in two-photon optics rate of joint detection counts, hence second order correlation functions, are measured. And while in classical optics intensities are the modulo-squared of electric fields, in two-photon optics second order correlation functions are the modulo-squared of the two-photon effective wavefunction. The two-photon effective wavefunction contains the coherent superposition of all the two-photon probability amplitudes that can lead to a joint photodetection. This is the link between classical Fourier optics and two-photon Fourier optics: the results are equivalent if the classical electric field are replaced by the two-photon probability amplitudes.

By using Eq. 2 and Eq. 3, the spatial part of the second order correlation function reduces to:

$$G^{(2)}(\boldsymbol{x}_1, \boldsymbol{x}_2) \propto |\sum_{\boldsymbol{q}} g_1(\boldsymbol{x}_1, \boldsymbol{q}) g_2(\boldsymbol{x}_2, -\boldsymbol{q})|^2 \tag{5}$$

where $\boldsymbol{x}_1$ and $\boldsymbol{x}_2$ are two-dimensional vectors in the transverse planes of detectors D_1 and D_2 respectively.

Let's consider, first, the setup in Fig. 1 in order to show how the which-slit information is mapped into the "ghost" imaging plane. For the sake of simplicity, let's work in one dimension just analyzing the horizontal transverse direction. For this setup, the Green's functions are:

$$g_1(x_1; q) \propto \Psi[q, -\frac{c}{\omega} d_A] \int dx_o T(x_o) e^{iqx_o} \Psi[x_1, \frac{\omega}{c} d'_A] e^{i \frac{\omega x_1 x_o}{c d'_A}}$$
$$g_2(x_2; q) \propto \Psi[q, -\frac{c}{\omega}(d_B - \frac{1}{\frac{1}{d'_B} - \frac{1}{f}})] e^{\frac{iqx_2}{1 - d'_B/f}} \Psi[x_2, \frac{c}{\omega} \frac{1}{d'_B - f}] \tag{6}$$

where the paraxial approximation and a source of infinite transverse size have been assumed. $\Psi(|\boldsymbol{q}|, \frac{\omega}{c} p) = e^{\frac{i}{2} \frac{\omega}{c} p |\boldsymbol{q}|^2}$ [24].

If the two-photon Gaussian thin lens equation is satisfied:

$$\frac{1}{d_A + d_B} + \frac{1}{d'_B} = \frac{1}{f} \tag{7}$$

and in particular the unitary magnification condition:

$$d_A + d_B = 2f$$
$$d'_B = 2f \tag{8}$$

the second order correlation function can be rewritten as

$$G^{(2)}(x_1, x_2) \propto |\int dx_o T(x_o) e^{i \frac{\omega}{c d'_A} x_1 x_o} \delta(x_o - x_2)|^2$$
$$\propto |T(x_2)|^2 \tag{9}$$

It is evident from the δ-function in Eq. 9 that every point of the plane of the double-slit is linked to a point in the "ghost" imaging plane that we labelled x_I: hence in the plane x_I of the two-photon image there is the information about the path followed by the signal photon in the plane x_o of the slit.

3.2 Reading or erasing the which-path information of the ghost imaging plane

In order to have the ability of reading or erasing the which-path information present at x_I it is possible to place a second lens L' in the plane x_I of the two-photon image and to detect the idler photon in the plane where the Fourier transform of the two-photon image is formed. It is known from Fourier analysis applied to optical signals that if we measure all the Fourier transform of the image we will still have all the information we had in the image plane, but if we detect only one point of such Fourier

transform plane, the information of the image plane will be inevitably erased.

The optical setup that implements such situation is depicted in Fig. 2: a lens L' of focal length f' is in the imaging plane and a pinhole P is located before detector D_2 in the Fourier transform plane of the image field distribution. In this case, the Green's function of one arm $g_1(x_1; q)$ is unchanged, while $g_2(x_2; q)$ becomes (notice that x_2 is in the plane of the detector D_2, and we will use x_I to indicate the transverse coordinate in the plane of the image):

$$g_2(x_2; q) \propto \Psi[q, -\frac{c}{\omega}(d_B + \frac{d'_B f}{f - d'_B})] \int d\, x_I\, e^{\frac{iqx_I}{1-d'_B/f}} \Psi[x_2, \frac{\omega}{cz}] e^{\frac{i\omega x_I}{cz}} \tag{10}$$

The second order correlation function is then:

$$G^{(2)}(x_1, x_2) \propto |\int dx_I T(x_I) e^{i\frac{\omega x_I}{c}[\frac{x_2}{z} + \frac{x_1}{d'_A}]}|^2 \tag{11}$$

In the case in which only one point (e.g. $x_2 = 0$) in the Fourier plane is considered (what we named *erasing* condition), the second order correlation function reads:

$$G^{(2)}_{erase}(x_1) \propto |\int dx_I T(x_I) e^{i\frac{cx_1 x_I}{\omega d'_A}}|^2 \propto |F_{\frac{\omega x_1}{cd'_A}}(T(x_I))|^2 \tag{12}$$

that in the case of a double-slit of slit width a and slit separation d becomes the usual interference diffraction pattern:

$$G^{(2)}_{erase}(x_1) \propto Sinc^2(\frac{\pi x_1 a}{\lambda d'_A}) Cos^2(\frac{\pi x_1 d}{\lambda d'_A}) \tag{13}$$

In the case in which all the photons arriving in the Fourier plane are detected (*reading* condition), the second order correlation function becomes:

$$G^{(2)}_{read}(x_1) \propto \int dx_2 |F_{\frac{\omega}{c}[\frac{x_1}{d'_A} + \frac{x_2}{z}]}\{T(x_I)\}|^2 = constant \tag{14}$$

that shows the absence of any interference pattern.

As we pointed out in the introduction, the interpretation of the quantum eraser results in terms of complementarity examination on a single photon is troubling. On the other hand, the straightforward calculation presented here can be intuitively captured if it is based on the concept of nonlocal two-photon amplitudes and their coherent superposition. In this sense, the physics behind entangled two-photon phenomena seems having no classical counterpart in electromagnetic theory. In order to help clarifying this physics, Klyshko proposed an "advanced-wave model"[20] that forces a classical counterpart of the concept of two-photon amplitudes and the associated two-photon optics. In his model, Klyshko considered the light to start from one of the detectors, propagate backwards in time until the two-photon source of SPDC and then forward in time towards the other detector. The two-photon source is thus playing the role of a mirror to keep the proper transverse momentum relation of the entangled photon pair. Fig. 2 is particularly suitable for Klyshko's picture: the which path information is carried by the advanced waves from the double-slit to the Fourier Transform plane of the ghost image according to the classical rules of Fourier optics. A straightforward calculation reveals that the Fourier Transform plane, referring to Fig. 2, is at a distance z from lens L' such that:

$$\frac{1}{d'_B - f} + \frac{1}{z} = \frac{1}{f'} \tag{15}$$

This equation has a ready explanation: it is a thin lens equation involving lens L' in which the object plane coincides with the focal plane of lens L. Therefore, if we read Fig. 2 from right to left, from the idler detector till the double-slit, we can provide another perspective on the optical interpretation of the phenomenon. The erasing condition is equivalent to having a point source and a lens system at a focal distance from it in such a way that only one momentum of propagation of the two-photon light is selected. It is then natural to observe an interference pattern from the double-slit because collimated radiation, with only one $\boldsymbol{k}$, is impinging on it. On the other hand, in the reading condition the situation is equivalent to having an extended source; as a result the radiation that impinges on the double-slit has all possible values of the momentum and each of the momenta will produce a slightly shifted interference-diffraction pattern. The total result, due to the incoherent sum of all such patterns, will be a constant.

The above two-photon picture helps establishing a connection between this eraser and the ghost interference effect first demonstrated by Strekalov et al. [25] as well as the erasure's idea by Dopfer et al. that similarly used the transverse correlations of SPDC even though it did not involve the transfer of the which-path information via imaging[10]. Using Klyshko's picture, even the puzzling physics of quantum erasure is trivial, which is the beauty of Klyshko's model.

4 Experiment

A sketch of the experimental setup is presented in Fig. **??**. A 5-mm type-II BBO crystal, cut for collinear degenerate phase matching was pumped by an Ar^+ laser at wavelength 457.9 nm. After passing the nonlinear crystal, the pump radiation was filtered out by a mirror with high reflection at the pump wavelength and high transmission at the wavelength of the signal and idler by an $RG715$ color glass filter. The signal-idler radiation was then split by a polarizing beam splitter; in the transmitted arm (A) a double-slit was placed at distance $d_A = 115mm$ from the crystal and in the far field zone ($d'_A = 1250mm$) a narrow bandpass filter (10 nm band centered at 916 nm)

was inserted in front of D_1, a single photon counting detector (Perkin Elmer SPCM-AQR-14) that was used to scan the transverse horizontal direction; in the reflected arm (B) a lens L of focal length $f = 500mm$ was placed at a distance $d_B = 885mm$ from the BBO crystal and a non polarizing beam splitter ($NPBS$) was at a distance $d_{NPBS} = 985mm$ from the lens L. Notice that the beam splitter $NPBS$ is the device at which the idler photon makes the random choice. In the output ports of $NPBS$ we built the two different ways of detecting the idler photons following the example of Fig. 4: in the transmitted arm a lens L'_T of focal length $f'_T = 250mm$ was at a distance $d_{L'} = 15mm$ from $NPBS$ and a very small pinhole P_T was placed at $z_T = 500mm$ from the lens just before coupling the radiation in a 4.5 m long multimode optical fiber (F_T); in the reflected arm a lens L'_R of focal length $f'_T = 50mm$ was at a distance $d_{L'} = 15mm$ from $NPBS$ and a completely open pinhole P_R was placed at $z_R = 55mm$ from the lens just before coupling the radiation in a 2 m long multimode optical fiber (F_R). The two optical fibers were then joined at a 2 to 1 fiber combiner and their output was filtered by a narrow bandpass filter (10 nm band centered at 916 nm) and measured by a single photon counting detector (Perkin Elmer SPCM-AQR-14). The output photocurrent pulses from the two photodetectors were finally sent to the "start" and "stop" inputs of a Time to Amplitude Converter (TAC) then connected to a MultiChannel Analyzer (MCA) and with a PC the coincidence counting rate in a desired window was measured.

Usually in delayed-choice quantum eraser experiments, each choice is associated with a different detector and therefore the two situations of no interference or recovered interference are obtained by counting coincidences with a separate measurement device. In our experiment we decided to use only one photo-detector D_2. Both transmitted and reflected photons at $NPBS$ were sent to D_2 with different optical delays (given by the different length of the fibers F_T and F_R). In this way we created histograms as in Fig. 4 that measure the second-order correlation function as a function of $t_2 - t_1$ and that calibrate the coincidence time window for the actual coincidence counting measurement: the first peak corresponds to the coincidence counts of D_2 with the reflected side of $NPBS$ (*reading* situation) while the second peak corresponds to the coincidence detections of D_2 with the transmitted side of $NPBS$ (*erasing* condition). The coincidence counting rate associated to each choice is then measured within the appropriate coincidence time window.

The curves in Fig. 4 carry another significant information. The FWHM of the curves is mainly determined by the response times of the detectors and measures the uncertainty with which we are able to determine the difference in time arrival between signal and idler photons $\Delta(t_2 - t_1)$. In order to achieve the delayed erasure condition, i.e. the choice of the idler photon and the detection of the signal photon at D_1 have to be space-like separated events; the optical path difference between the crystal and the $NPBS$ (where the choice is randomly made) has to be bigger that the distance from the crystal to detector D_1 of a quantity larger than $\Delta(t_2 - t_1)$. In this case $\Delta(t_2 - t_1) \sim 1ns$, while the difference in path lengths $[(d_B + d_{NPBS}) - (d'_A + d_A)]/c \sim 1.7ns$, therefore we can be sure that the choice is made after the detection of the signal photon at detector D_1.

The experimental results are shown in Fig. 5 and Fig. 6. They refer to two different double-slits: one with slit width of $a = 150\mu m$ and slit separation $d = 470\mu m$ and the other with slit width of $a = 100\mu m$ and slit separation $d = 250\mu m$. In the graphs both the *erasing* condition measurement (empty circles) and the *reading* condition measurements (filled squared) are shown. As expected, when we read the which-path information, we do not see any interference pattern while when we erase such information the experimental data agree with the expected interference-diffraction of the double-slits. The visibilities of both interference patterns are very high (85% and 95% respectively) and only limited by the finite size ($\sim 200\mu m$) of detector D_1.

Let us now point out some additional characteristics of the experimental setup. (1) The double-slit has to satisfy the condition $\Delta\theta \gg \lambda/d$ in order to avoid the existence of any first order interference-diffraction pattern. From the tuning curves of the BBO crystal we computed the divergence of the SPDC radiation to be around $\Delta\theta \sim 27mrad$. For this reason we chose two different double-slits, one with $\lambda/d \sim 3mrad$ and the other with $\lambda/d \sim 1.5mrad$. (2) The two lenses L'_T and L'_R are placed in the plane where the two-photon image of the double-slit is formed as described in the theory section. Notice, in fact, that the distance from the slit, back to the crystal and forward to the lens L, i.e. $d_A + d_B$ is exactly equal to $2f$; also, the distances from the lens L to the two lenses L'_T and L'_R, i.e. $d'_B = d_{NPBS} + d_{L'}$ is again equal to $2f$. Therefore such distances satisfy the two-photon Gaussian thin lens equation with unitary magnification of Eq. 7 and Eq. 8. (3) We used two different lenses L' in order to better achieve the *reading* and *erasing* condition mentioned in the theory section. In the transmitted arm of $NPBS$, the focal length of L'_T is large, therefore a small pinhole is a good approximation of taking only the central point of the Fourier plane; on the other hand, in the reflected arm the focal length of L'_R is short, therefore a completely open pinhole P_R of diameter $\sim 1cm$, is a very good approximation of detection of all the Fourier plane.

5 Conclusion

The key idea of the eraser is to transfer the which-path information to a distant location via a two-photon "ghost" image and then *read* or *erase* the path information in its Fourier transform. Therefore, the result of this quantum eraser can be viewed in terms of continuous variables of position and momentum. This aspect is interesting given the recent interest in continuous variable entanglement for quantum information processing[17,26,27]. Using a double slit in the actual experiment and therefore proving Eq. 13 was a matter of convenience and clarity. However, the observed interference-diffraction pattern is experimental ev-

idence of the general result in Eq. 12. Therefore, there is no restriction, in principle, to extend the present idea to multi-slits (paths) or even continuous spatial modulation.

Having demonstrated a quantum eraser via two-photon ghost imaging with a Fourier transform approach shows that ghost imaging schemes coherently transfer the optical information between two distinct arms of a setup. This property might be useful because it shows the possibility to implement phase operations, or Fourier manipulations in a nonlocal fashion to improve the optical performances of imaging schemes.

From a fundamental point of view, we have demonstrated a new scheme for delayed choice quantum eraser. This new eraser has probed all the interesting physics proposed by Scully and Druhl. The experiment, from a different perspective, demonstrates and questions two of the most intriguing fundamental concepts of quantum theory: complementarity and entanglement.

As for the complementarity, for the first time, a delayed choice quantum eraser is demonstrated in which the choice to erase or not erase is realized truly at random in only one photo-detector. In many previous experiments the interference or no interference situations involved basically different experiments and/or different experimental runs. Some of the other previous quantum erasers did not involve different experimental realizations, but anyway two different measurement devices were associated to the erasing and not erasing conditions. In our experiment all the photons, belonging to either choice, arrive to the same photo-electric device truly at random. This aspect is very interesting because the experimental conditions associated with the different choices are very similar and therefore it is not trivial to establish where the measurement, hence the collapse of the wave function, occurs.

As for the entanglement, this experiment has strikingly shown a fundamental point that is often forgotten: for entangled photons it is misleading and incorrect to interpret the physical phenomena in terms of independent photons. On the contrary the concept of "biphoton" wavepacket has to be introduced to understand the nonlocal spatio-temporal correlations of such kind of states. Based on such a concept, a complete equivalence between two-photon Fourier optics and classical Fourier optics can be established if the classical electric field is replaced with the two-photon probability amplitude. The physical interpretation of the eraser that is so puzzling in terms of individual photons' behavior is seen as a straightforward application of two-photon imaging systems if the nonlocal character of the biphoton is taken into account by using Klyshko's picture.

The authors thank M.H. Rubin for everyday help and discussions and M.O. Scully and C.O. Alley for the encouragement of conducting this experiment. This research was supported in part by ARO and the CASPR program of NASA.

References

1. M.O. Scully and K. Druhl, Phys. Rev. A **25**, 2208 (1982).
2. Y. Aharonov and M.S. Zubairy, Science **307**, 875 (2005).
3. S.P. Walborn, M.O. Terra Cunha, S. Padua, C.H. Monken, American Scientist **91**, 336-343 (2003).
4. N. Bohr, Naturwissenschaften **16**, 245 (1928).
5. *Quantum theory and measurement*, edited by J.A. Wheeler and W.H. Zurek (Princeton University Press, Princeton, NJ,1983).
6. C.O. Alley, O. Jacubowicz, and E.C. Wickes, in *Proceedings of the Second International Symposium on Foundations of Quantum Mechanics in the Light of New Technology*, edited by M. Namiki et al. (Physical Society of Japan, Tokyo, 1986), p. 36.
7. P. G. Kwiat, A. M. Steinberg, and R. Y. Chiao, Phys. Rev. A **45**, 7729-7739 (1992).
8. T.J. Herzog, P.G. Kwiat, H. Weinfurter, and A. Zeilinger, Phys. Rev. Lett. **75** 3034 (1995).
9. S. Durr, T. Nonn, and G. Rempe, Nature (London) **395**, 33 (1998).
10. B. Dopfer, PhD. Thesis, Universtat Innsbruck (1998).
11. P.D.D. Schwindt, P.G. Kwiat, and B.-G. Englert Phys. Rev. A **60** 4285 (1999).
12. Y.H. Kim, R. Yu, S.P. Kulik, Y. Shih and M.O. Scully, Phys. Rev. Lett. **84**, 1 (2000).
13. T. Tsegaye, G. Bjork, M. Atature, A. V. Sergienko, B. E. A. Saleh, and M. C. Teich, Phys. Rev. A **62**, 032106 (2000).
14. P. Bertet, S. Osnaghi, A. Rauschenbeutel, G. Nogues, A. Auffeves, M. Brune, J.M. Raimond and S. Haroche, Nature **411**, 166 (2001).
15. A. Trifonov, G. Bjork, J. Soderholm and T. Tsegaye, Eur. Phys. J. D **18**, 251-258 (2002).
16. S. P. Walborn, M. O. Terra Cunha, S. Padua, and C. H. Monken, Phys. Rev. A **65**, 033818 (2002).
17. U.L. Andersen, O. Glockl, S. Lorenz, G. Leuchs, and R. Filip, Phys. Rev. Lett. **93**, 100403 (2004).
18. Y. H. Shih, Rep. on Progress in Physics, **66**, No. 6, (2003).
19. T.B. Pittman, Y.H. Shih, D.V. Strekalov, and A.V. Sergienko, Phys. Rev. A **52**, R3429 (1995).
20. D.N. Klyshko, Phys. Lett. A **128**, 133 (1988); Phys. Lett. A **132**, 299 (1988); A.V. Belinskii and D.N. Klyshko, JETP **78**,259 (1994).
21. A.F. Abouraddy, B.E.A. Saleh, A.V. Sergienko, M.C. Teich, J. of Opt. Soc. Am. B **19**, 1174 (2002).
22. R.J. Glauber, Phys. Rev. **130**, 2529 (1963) ; U.M. Titulaer and R.J. Glauber, Phys. Rev. **140**, B676 (1965).
23. D.N. Klyshko *Photons and Nonlinear Optics* Gordon and Breach Science Publishers (Amsterdam 1988).
24. M. H. Rubin, Phys. Rev. A **54**, 5349, (1996).
25. D.V. Strekalov, A.V. Sergienko, D.N. Klyshko and Y.H. Shih, Phys. Rev. Lett. **74**, 3600 (1995).
26. R. Filip, Phys. Rev. A **67**, 042111 (2003).
27. P. Marek and R. Filip, Phys. Rev. A **70**, 022305 (2004).

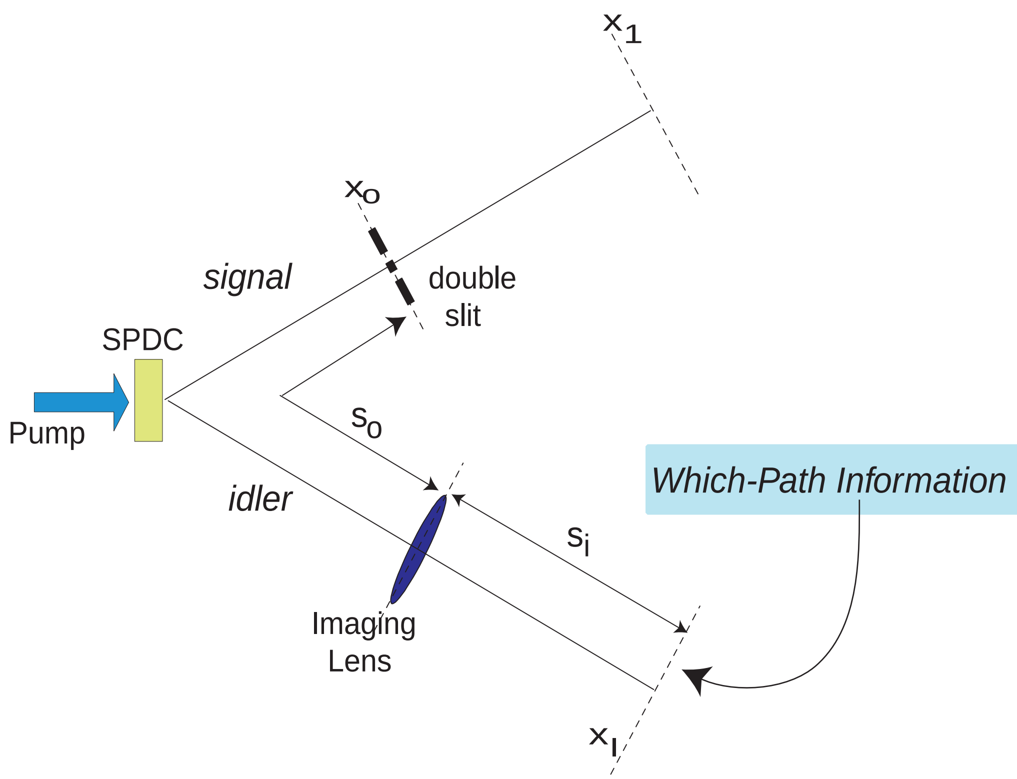


Fig. 1. Schematic of the quantum erasure: the double-slit in the plane x_o is imaged in the plane x_I because of the quantum correlations of entangled photon pairs. Hence the which-path information is mapped onto the two-photon imaging plane.

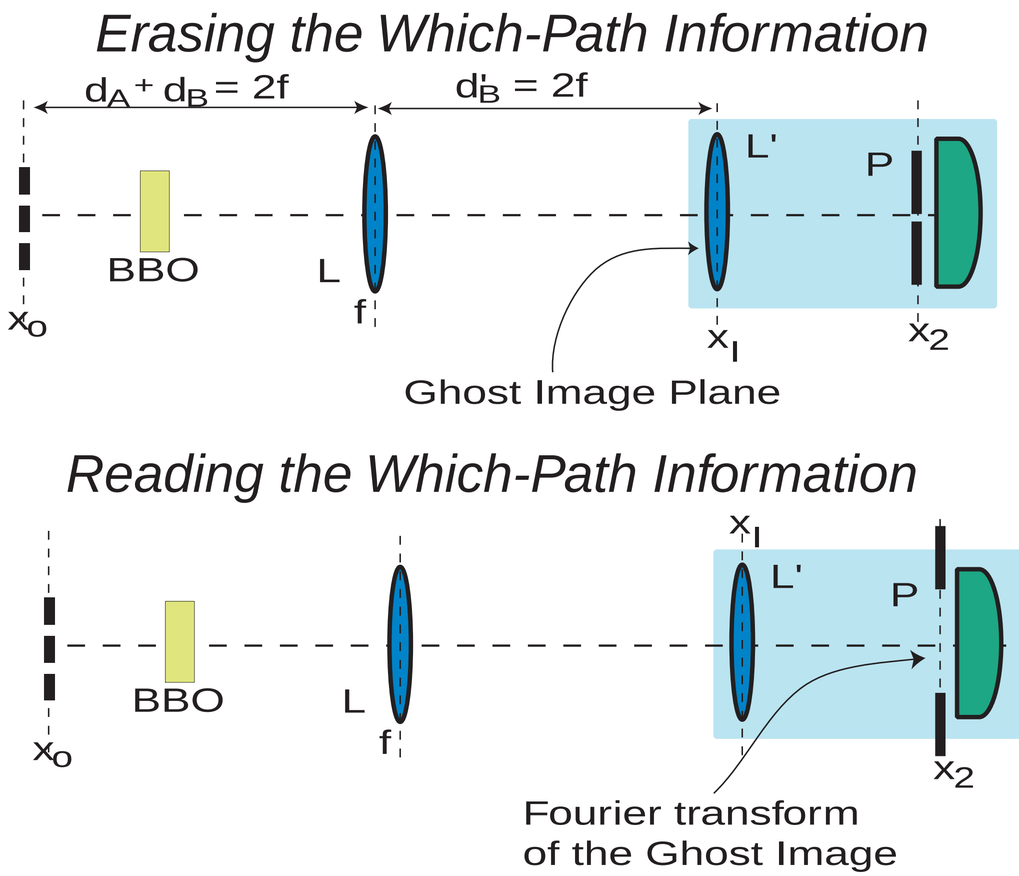


Fig. 2. Klyshko's picture of the two-photon imaging setup showing the two choices that we named *erasing* and *reading*. In both cases a lens L is placed in the plane of the two-photon image and the detector is placed in the plane of the Fourier transform of the two-photon image. In part (a) the entire Fourier transform is collected by D_2. In part (b) only the central part of the Fourier transform is detected by D_2.

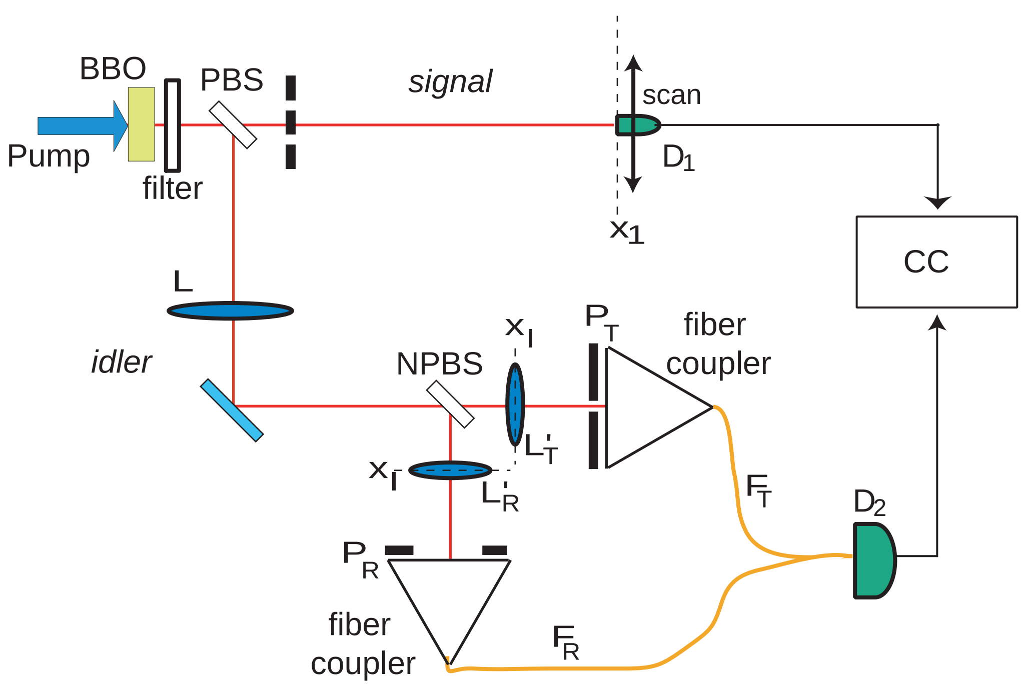


Fig. 3. Schematic of the experimental setup.

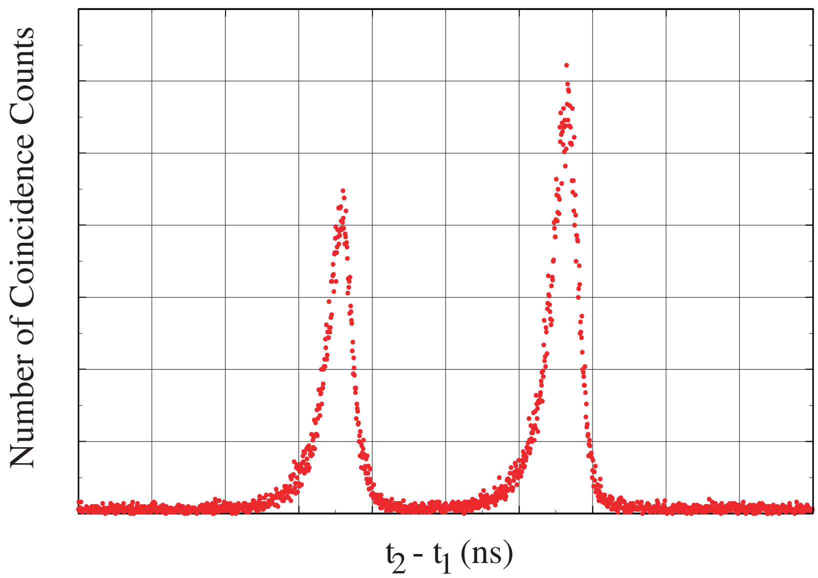


Fig. 4. Typical MCA distribution. The two different way of detecting idler photon are time "encoded" by using two multimode optical fibers of different length; hence in the MCA pattern the two peaks correspond to the two different situations.

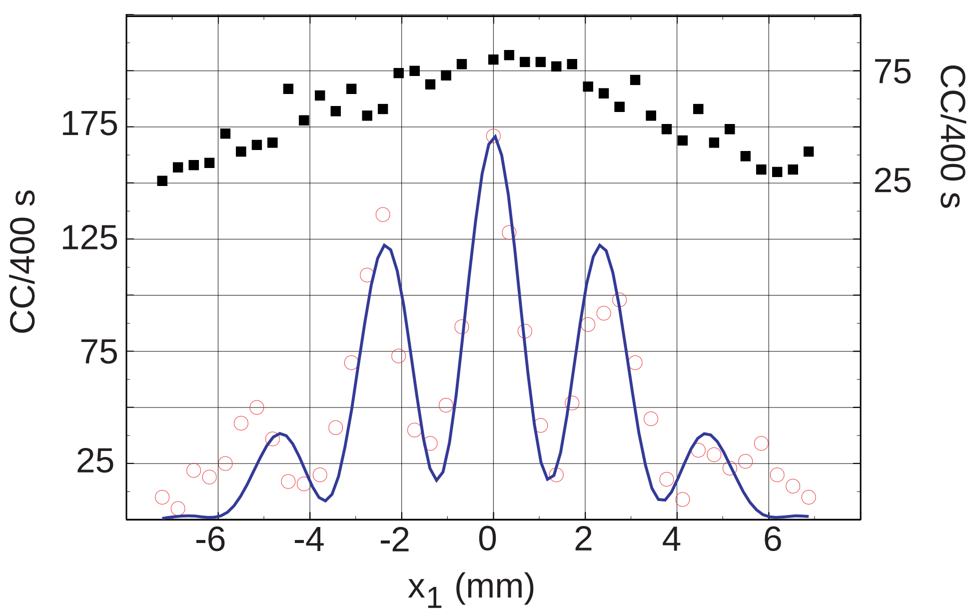


Fig. 5. Experimental results for a double-slit of slit width $a = 150\mu m$ and slit separation $d = 470\mu m$. The filled squares show the coincidence count pattern obtained in the *reading* situation, while the empty circles indicates the pattern obtained in the *erasing* situation. The solid line is the theoretical expectation of a 85% visibility interference-diffraction pattern.

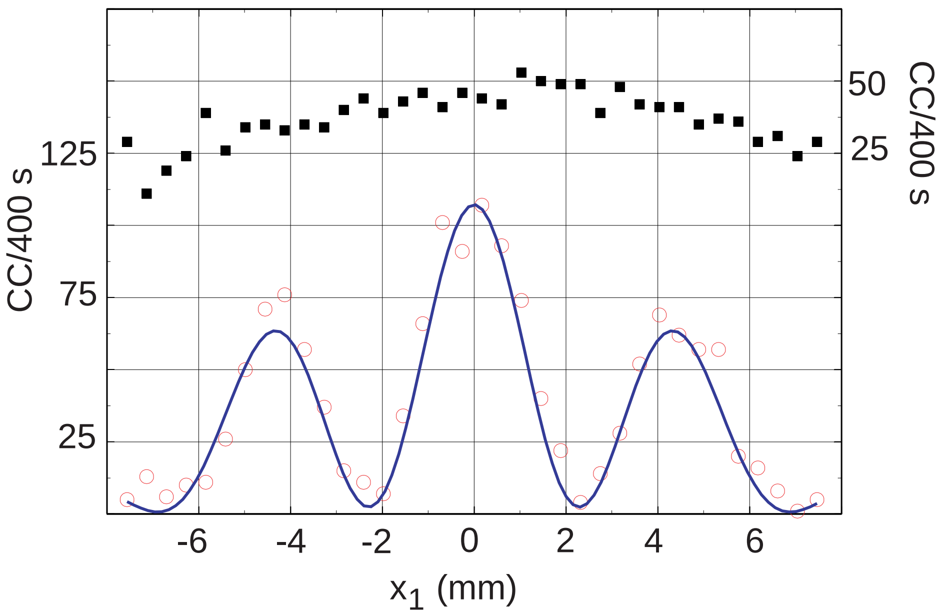


Fig. 6. Experimental results for a double-slit of slit width $a = 100\mu m$ and slit separation $d = 25\mu m$. The filled squares show the coincidence count pattern obtained in the *reading* situation, while the empty circles indicates tha pattern obtained in the *erasing* situation. The solid line is the theoretical expectation of a 95% visibility interference-diffraction pattern.